

Investigation and Development of Sn-Zn System as an Alternative to Sn-Pb Eutectic Toxic Solder Alloy

Shakib Alsowidy*, Esmail Abdo Mohammed Ali, and Adel Hassaan Alsaoraky

Department of Physics, Sana'a University, Sana'a, Yemen

*Corresponding author: Shakib Alsowidy, Department of Physics, Sana'a University, Sana'a, Yemen, Tel: 967777472598; E-mail: dralsowidy@gmail.com

Received date: October 06, 2021; Accepted date: October 20, 2021; Published date: October 27, 2021

Citation: Alsowidy S, Mohammed Ali EA, Alsaoraky AH (2021) Investigation and Development of Sn-Zn System as an Alternative to Sn-Pb Eutectic Toxic Solder Alloy. J Mater Sci Nanomater 5: 140.

Copyright: © 2021 Alsowidy S, et al. This is an open-access article distributed under the terms of the Creative Commons Attribution License, which permits unrestricted use, distribution, and reproduction in any medium, provided the original author and source are credited.

Abstract

Variations of melting temperature and microstructure of six compositions based on Sn-9wt% Zn eutectic containing small additions of copper from 0.2wt% to 1.0wt% were investigated. These six compositions of Sn-9wt%-x wt% Cu ($x = 0, 0.2, 0.4, 0.6, 0.8, 1.0$) have been prepared by melting accurately weight amounts of pure metals of 99.99% in a furnace under vacuum. The possible phase transformations that may be occurred in the samples were monitored by recording thermal energy flow as a function of time and temperature using Differential Scanning Calorimetry Analysis (DSCA). From DSCA, it has been found that there are a slightly change in melting point and pasty range and increase with increasing Cu-content. The variations in microstructure with copper content have been determined using X-Ray Diffraction Analysis (XRDA). The obtained x-ray diffraction patterns show that new different phases have been formed in the ternary alloys and the crystalline size increases with increasing Cu-content. These changes in melting point and particle size were attributed to a number of factors including the formation of Cu_5Zn_8 IMC and Sn/Zn hypoeutectic phases in the structure after copper addition. The mechanical response of the binary and ternary alloys has been determined and correlated to the variation in microstructure and thermal characteristics

Keywords: Lead-free solder; Eutectic alloy; Nanoparticle size; Microstructure; Microstrain; Intermetallic compounds

Introduction

All the time in the history of electronics packaging, eutectic Sn-Pb has been the most extensively used soldering alloy. This solder alloy has a relatively low melting temperature (183°C), excellent ductility and creep rates, and compatibility with most substrates and devices. However, despite the advantages of Sn-Pb as an eutectic solder alloy, it has been prohibited in many countries due to environmental and health concerns. In July 2006, European Commission's has approved banning the use of lead in electronics in European Union countries. Furthermore, several Japanese electronics manufacturers have successfully created a market differentiation based on green products that use Pb-free solders. So, the conversion to Pb-free solders in the electronics industry appears imminent. As a result, efforts to develop alternatives to Pb solders have been continuously increasing in recent years. There is a number of characteristics that plays a vital role in substitution of Sn/Pb eutectic solder, such as

- Environmental issues related to the toxicity.
- Lower melting temperature.
- Adequate tensile strength.
- Stability in microstructure during operation.
- Low cost.
- availability in sufficient quantities as concerns the base metals.

All these characteristics depend on the solder constituent and affected by the solder composition. The majority of the lead free alloys are Sn-based alloys. Sn-based alloys involving elements such as Ag, Cu, Bi, and Zn have been recognized as promising candidates. In

fact, Sn-rich lead free alloys have occupied more than 80% in the wave solder market share and more than 90% in the reflow solder market share. All alternatives to the standard eutectic tin-lead solder investigated so far are based on tin alloys with a tin content significantly over 90wt. % in combination with copper, silver, antimony, bismuth, or zinc. Recently, Sn-Zn binary solder alloy is one of the most alloys recommended as an alternative to Sn-Pb eutectic solder alloys [1]. This is due to the following features:

- Sn and Zn are low cost metals.
- Lower melting temperature close to Sn-Pb alloys.
- Mechanical characteristics is better than that of Sn-Pb alloys.
- More structure stability.
- Non-toxic.

Sn-9Zn eutectic solders have limited commercial viability due to its serious oxidation and corrosion problems. During soldering the metal, the active zinc atoms may get oxidized and create voids in the matrix. The zinc oxide formed on the surface of solder alloy during soldering prevents the solder from wetting and then bad joining may be expected between metals. Due to these and according to literature review all these problems can be prevented by adding a third element, such as copper, aluminum, or bismuth to the binary solder system. Thus the addition of Cu as a reactive element into Sn 9Zn binary alloy may improve its oxidation resistance. In other hand, copper addition as a third element may change the microstructure and mechanical characteristics and melting temperature of Sn-9Zn binary eutectic solder alloy. In this study, the effect of various amount of copper content up to 1wt% on the melting temperature, microstructure and

mechanical characteristics of Sn-9wt% Zn-xwt% Cu alloys, will be investigated before and after addition.

Experimental Techniques

The lead-free of six compositions Sn - 9wt% Zn - xwt% Cu (x=0, 0.2, 0.4, 0.6, 0.8, 1.0) were prepared from Sn, Zn, and Cu with purity of 99.99% by vacuum melting. The experimental weighted compositions of the prepared alloys are shown in Table 1. The cast ingots were cold drawn to wire samples of 0.8 mm in diameter and 30 mm length. Thermal annealing at 100°C has been carried out for six hours and then slow cooling to room temperature with cooling rate of 1°C/min. This produces samples containing fully precipitated phases and avoids inhomogeneity structure of the six samples. Thermal properties of six samples were tested using the technique of DSC and done by NETZSCH STA 449 F3 Jupiter. The samples of approximate weight of 0.9 mg were heated to 250°C with a constant rate of 10°C/min. The effects of copper addition on microstructure have been determined by x-ray diffraction using XD-2 Powder x-ray Diffractometer with CuK radiation with a wavelength of 1.54056 Å. Grain size and dislocation density were calculated and correlated to the copper content in the system. In order to determine the relation between mechanical strength and copper content in the system, tensile test was performed for six samples under room temperature using floor-standing electromechanical universal testing machine CMT4000 [2]. Ultimate tensile strength, elongation and creep rates have been calculated as a function of Cu-content. According to the fact that any change in microstructure of the material reflects on a variation of its properties, the effects of Cu-content on mechanical strength have been calculated and correlated to the microstructure observation.

Sample no	Alloys	Sn	Zn	Cu
1	Sn-9Zn	91	9	-
2	Sn-9Zn-0.2Cu	90.8	8.98	0.2
3	Sn-9Zn-0.4Cu	90.6	8.96	0.4
4	Sn-9Zn-0.6Cu	90.4	8.94	0.6
5	Sn-9Zn-0.8Cu	90.2	8.92	0.8
6	Sn-9Zn-1.0Cu	90.1	8.9	1

Table 1: Chemical composition of manufactured alloys (wt. %).

Results and Discussion

Differential scanning calorimetry analysis (DSCA)

It is known that, in soldering process, the melting point of the solder determine the maximum operating temperature of the system and the minimum processing temperature its component must survive. Due to the packaging density of electronic components in the last years, melting point, solidus and liquidus temperatures are considered very important thermal properties in evaluating reliability of electronic components. To determine these properties and other possible thermal reactions, Differential Scanning Calorimetry Analysis (DSCA) has been carried out over the temperature range from 25 to 250°C as shown in Figure 1. This Figure shows the superimposed curves of DSC obtained of the six Sn-Zn-Cu alloys. These DSC curves concerned peak and shoulder near the peak for binary and ternary

solders, respectively. The peak represents the melting temperature of the Sn-Zn eutectic composition and the shoulder represents the melting temperature of ε-Cu₅Zn₈ IMC. From DSC curve it can be seen that there is shifting between solidus and liquidus points and increase with increasing copper content. These points represent the beginning and ending of the phase transition (melting), respectively. The beginning and ending of this phase transition are moved to slightly larger temperature by the increase copper content. The melting, solidus, and liquidus temperatures for six compositions have been extracted from the DSC curves and given in Table 2. Furthermore, the reduction in Zn content in the system results change in the Sn-Zn eutectic composition. This means formation of Sn-Zn hypoeutectic structure. The melting point of this hypoeutectic is larger than that of Sn-Zn eutectic, and then the gap between T_{solidus} and T_{liquidus} increases with increasing copper content in the solder as can be seen from the Sn-Zn phase diagram shown in Figure 2. This result is in well agreement with a previous study which decided that the small addition of Cu into Sn-Zn alloy causes larger melting point of the system. From Sn-Zn phase diagram it is clear that there is no IMCs or new different phases are found other than Sn rich phase and Zn rich phase [3].

Sample no	Sample	Ts (°C)	TL (°C)	TE (°C)
1	Sn-9Zn	197.8	205.2	200
2	Sn-9Zn-0.2Cu	197.8	205.5	200.2
3	Sn-9Zn-0.4Cu	198.3	208.5	203.3
4	Sn-9Zn-0.6Cu	198.12	208.4	203.2
5	Sn-9Zn-0.8Cu	198.1	208.4	202.8
6	Sn-9Zn-1.0Cu	198	208.32	203

Table 2: Melting, solidus, and liquidus temperatures of six samples examined.

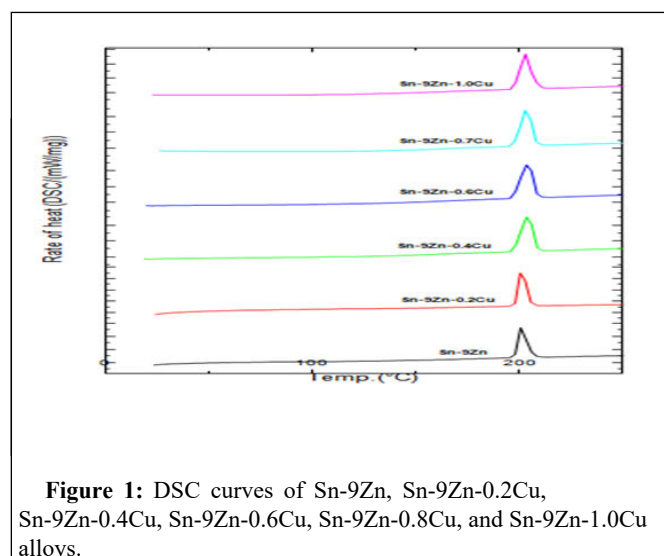


Figure 1: DSC curves of Sn-9Zn, Sn-9Zn-0.2Cu, Sn-9Zn-0.4Cu, Sn-9Zn-0.6Cu, Sn-9Zn-0.8Cu, and Sn-9Zn-1.0Cu alloys.

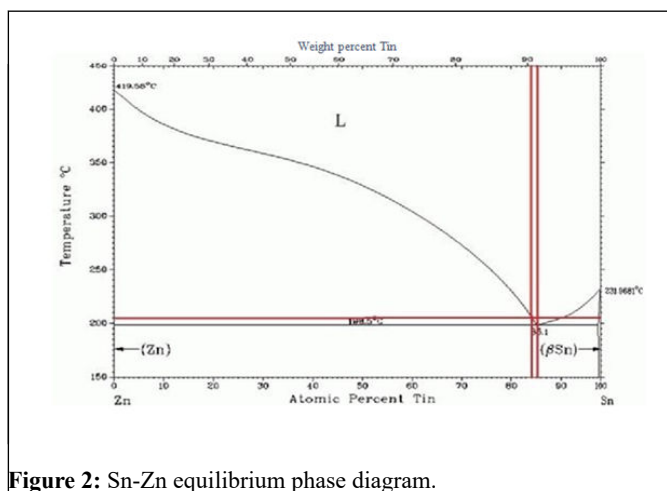


Figure 2: Sn-Zn equilibrium phase diagram.

According to the Cu-Sn and Cu-Zn phase diagrams, as temperature increased, there is no dissolution observed of copper into Sn while very small part of copper dissolves into Zn phase as reaction time increased forming α -Zn solid solution phase. According to the lever rule principle, this solid solution phase decreases in amount and nucleation and growth of ϵ - Cu_5Zn_8 IMC will continue as added more copper content in the system. Because the greater reactivity of Zn, this reaction continues without formation any Sn-Cu compounds until all free Zn phase is consumed. This result can be observed from XRD pattern shown in the next section. This result is in well agreement with the previous work performed by Rahman et al which reported that the small additions of copper into Sn-Zn alloy are forming only Cu_5Zn_8 phase in the system, and the higher Cu-content means the higher Cu_5Zn_8 IMC concentration. This causes significant increase in the liquidus temperature shown in Figure 3. The precipitation process of ϵ - Cu_5Zn_8 IMCs in the eutectic structure will be expected as can be observed from the XRD patterns and arising time of complete melting with copper content. The same behavior has been presented in literature.

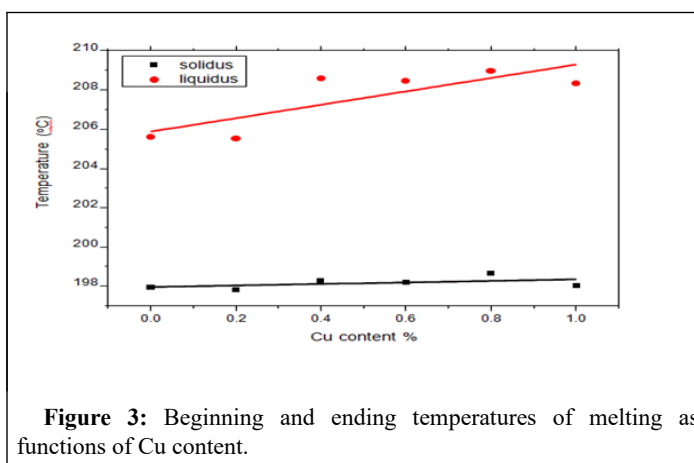


Figure 3: Beginning and ending temperatures of melting as functions of Cu content.

Due to the ϵ - Cu_5Zn_8 IMC, which the melting point is higher than the melting point of the eutectic Sn-Zn alloy, there is incomplete melting at eutectic temperature. This means that the IMC decelerates the transformation from solidus to liquidus and then the activation thermal energy required to melting has long time than in Sn-9Zn alloy. The time interval required to complete melting has been examined using DSC analysis for Sn-9Zn and Sn-9Zn-1Cu compositions as can be shown from Figure 4. It can be seen that the time interval required

to complete melting of Sn-9Zn-xCu composition is more than that of Sn-9Zn binary composition. This can be observed in significant decrease of creep rate as shown from Figure 5 and then better creep resistance.

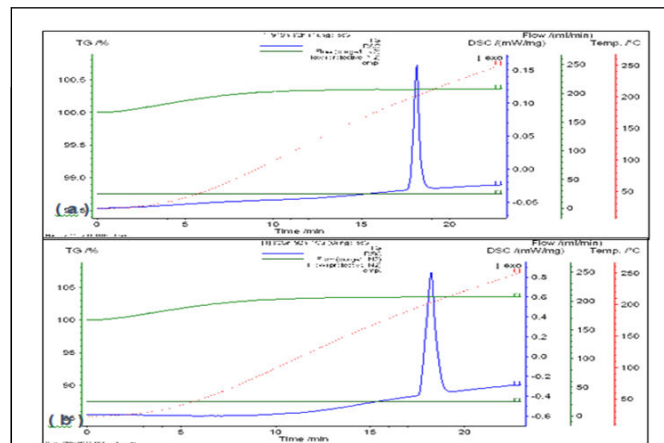


Figure 4: Variation of thermal energy flow with time for (a) Sn-9Zn and (b) Sn-9Zn-1Cu.

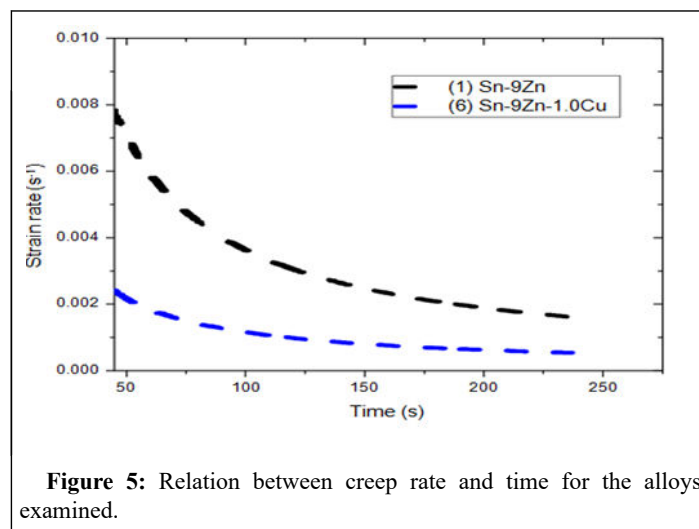


Figure 5: Relation between creep rate and time for the alloys examined.

Microstructure characteristics

XRD patterns and phase identification: The x-ray diffraction is a common characterization technique which is used to determine phases that found in the metal alloys. In order to determine the various phases in the six alloys, structure analysis using x-ray diffraction method has been performed using XD-2 Powder X-Ray Diffractometer, china. The diffraction pattern obtained is shown in Figure 6. The two phases β -Sn and α -Zn are the main constituents and clearly observed in these patterns. Since the maximum amplitude of the wave reflected by a set of N parallel atomic planes is proportional to N, the maximum intensity is proportional to N^2 . This means that the reflected intensity is proportional to the thickness or size of the crystal. Due to the large amount of tin element in the solder composition, Sn is nearly nine times Zn, the Tin Peaks are more prevalent than zinc Peaks. This difference can be seen very clearly by the differences in peak intensities between tin and zinc elements. According to Sn-Zn phase diagram, Figure 2 there is no interaction between them and the solid

solubility of one in each other is very limited. Therefore, there are no new phases expected in the system. The obtained diffraction patterns have been compared with standard powder diffraction data (pdf) using search/match process of measured data with appropriate reference file using jade software. The best matched diffraction patterns are marked and shown in Figure 6 for six samples [4]. It can be seen that the effect of Cu-content on intensity of all Sn peaks is not significant and there is no appearance of Cu-Sn IMCs phases while the intensity and peak broadening of all Zn peaks have been changed. It can be seen that the peak intensities of α -Zn phase decrease with increasing Cu-content. New Cu-Zn IMC phase has been produced as a result of chemical reaction between copper and zinc. According to Cu-Zn phase diagram and S/M process, this IMC is Cu_5Zn_8 . The density of this compound increases as Cu-content increased and causes a higher intensity peaks as can be seen from Figure 6. However, formation of Cu_5Zn_8 compound reduces Zn content and improves the formation of Sn/Zn hypoeutectic structure in ternary systems, Figure 2.

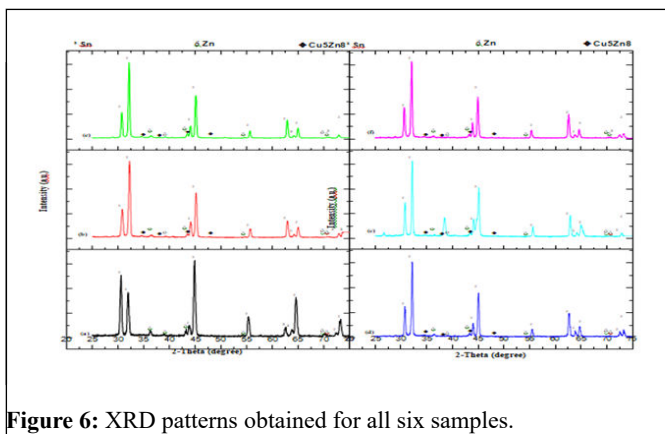
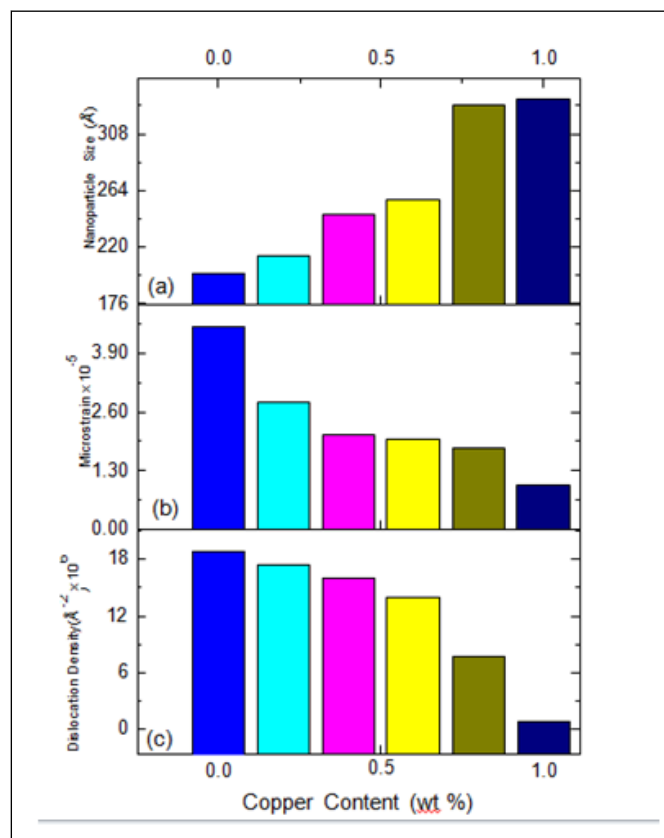


Figure 6: XRD patterns obtained for all six samples.

Grain Size and grain growth: It is known that the zinc atoms in Sn-matrix phase migrate towards Sn-grain boundaries and limiting their mobility and thus inhibit growth of grains. This is found and reported by various literatures. It has been found that the addition of zinc into tin decreases grain size of β -Sn phase. The same behavior has been reported by El-Dally et al. In that research, the effect of zinc addition on microstructure of Sn-Pb alloy was investigated and zinc atoms appeared to locate on grain boundaries of β -Sn and suppress grain growth of β -Sn phase. The tendency of zinc precipitates to site in grain boundaries of Sn was large and decrease with increasing Deformation temperature. This distribution of zinc precipitates suppress grain growth of β -Sn matrix. The copper addition into Sn-9Zn eutectic alloy produces CuZn IMCs. Increasing Cu-content increases the size of IMCs and reduce the Zn content in the eutectic composition. According to Zn-Cu phase diagram, as the Cu-content increase the amount of Cu_5Zn_8 IMC increases and the Zn content decreases. As copper content decrease, the higher amount of the precipitated α -Zn has resulted in more distinct peaks of this phase in its diffraction patterns. The width of diffraction curve increase as the thickness of the crystal decrease, the crystallite size D and lattice strain ϵ have been followed by the analysis of XRD pattern and by using the following Scherrer formula.



Where (β) is the diffraction rays breadth, (θ) is the Bragg's angle and (λ) is the wavelength of X-ray used. In order to obtain (D) and (ϵ) , the relation between $\beta \cos \theta$ and $2 \sin \theta / \lambda$ should be plotted. In order to verify the effects of copper addition on the microstructure of Sn-Zn eutectic solder alloy, the variations of nanoparticle size and microstrain have been calculated using equation (1) and plotted with Cu-content as can be seen from Figure 7, it can be seen that the particle size increases gradually with increasing Cu-content until reach 335 Å at 1wt% Cu. Due to the formation of Sn hypoeutectic, the dislocation inhalation may be expected at the grain boundaries of β -Sn phase and therefore decreasing in microstrain as shown from Figure 7. Dislocation density as a function of Cu-content is given. It can be seen that there is a reduction in dislocation density as more copper added.

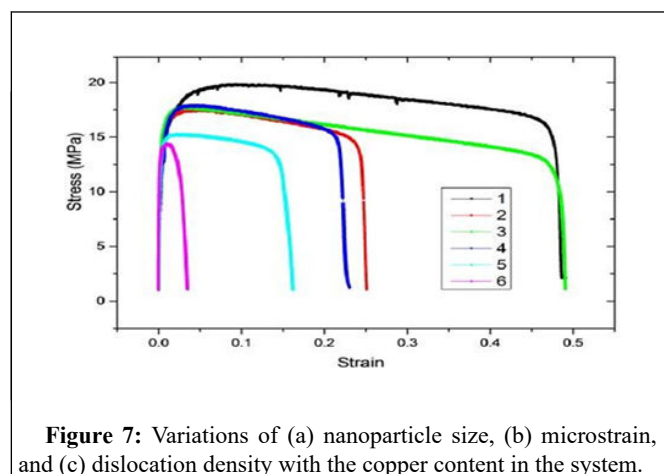


Figure 7: Variations of (a) nanoparticle size, (b) microstrain, and (c) dislocation density with the copper content in the system.

The effects of dislocations inhalation can be observed in tensile test shown in Figure 8. This figure shows the stress strain curves for six samples deformed at room temperature and 1 atmospheric pressure. The variations of UTS and elongation of six samples have been extracted from these stress - strain curves and given in Table 3. It can be seen that UTS decreases as the copper content increases. All UTS values obtained are better than that of Sn-Pb eutectic solder. In order to correlate between mechanical test and microstructure, the slope of the plastic region of six curves has been calculated and also given in the Table 3. The negative slope of this plastic region is an indication to work-softening process and then the structure recrystallization will be occurred. As can be seen this slope increases as Cu-content increased. This is due to inhalation of dislocations which result in increasing of crystallinity of microstructure. Thus, the grain growth is attributed to the formation of Cu₅Zn₈ IMC and Sn-hypoeutectic phases including dislocation inhalation and improvement of the mobilities of Sn grain boundaries [5].

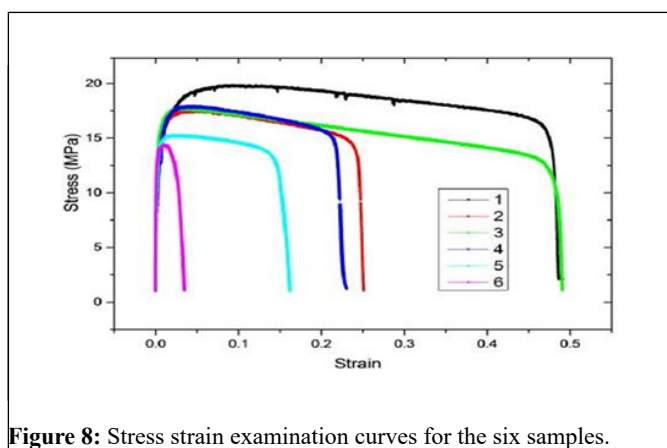


Figure 8: Stress strain examination curves for the six samples.

Sample no	Sample	UTS (MPa)	Elongation (%)	Slop of work softening (MPa)
1	Sn-9Zn	19.7	49	7.37
2	Sn-9Zn-0.2Cu	17.75	25	11.5
3	Sn-9Zn-0.4Cu	17.4	49	10.5
4	Sn-9Zn-0.6Cu	17.9	23	13.2
5	Sn-9Zn-0.8Cu	15.3	16	13
6	Sn-9Zn-1.0Cu	14.5	4	98

Table 3: The variations of UTS and elongation of six samples.

Conclusion

The changes in the eutectic point TE, liquidus point TL, solidus point TS, ultimate tensile strength UTS, nanoparticle size and dislocation density of Sn-9Zn eutectic solder were investigated as a function of Cu-addition.

The results obtained from the present study can be summarized as follows:

- The melting temperature and pasty range slightly increased with increasing Cu-content.
- All values of ultimate tensile strength UTS obtained from the stress-strain measurements of Sn-Zn-xCu are better than that of Sn-Pb eutectic solder.
- New phase of Cu₅Zn₈ IMC was nucleated and its amount increased with increasing Cu-content.
- The particle size has been increased from 200 Å for Sn-9Zn to 300 Å for Sn-9zn-1.0Cu.
- From the microstructure observation there are no strange effects of copper addition on the stability of microstructure while slightly recrystallization of microstructure has been observed as a result of dislocation inhalation in β-Sn grain boundaries.

References

1. Hammam M, Allah FS, Gouda ES, El Gendy Y, Aziz HA (2010) Structure and properties of Sn-9Zn Lead-free solder alloy with heat treatment. *Engineering 2*: 172.
2. Noh BI, Choi JH, Yoon JW, Jung SB (2010) Effects of cerium content on wettability, microstructure and mechanical properties of Sn-Ag-Ce solder alloys. *J Alloy Compound 499*: 154-159.
3. Islam RA, Wu BY, Alam MO, Chan YC, Jillek W (2005) Investigations on microhardness of Sn-Zn based lead-free solder alloys as replacement of Sn-Pb solder. *J Alloy Compound 392*: 149-158.
4. Islam MN, Chan Y, Rizvi MJ, Jillek W (2005) Investigations of interfacial reactions of Sn-Zn based and Sn-Ag-Cu lead-free solder alloys as replacement for Sn-Pb solder. *J Alloy Compound 400*: 136-144.
5. El-Daly AA, Swilem Y, Makled MH, El-Shaarawy MG, Abdraboh AM (2009) Thermal and mechanical properties of Sn-Zn-Bi lead-free solder alloys. *J Alloy Compounds 484*: 134-142.